Applied Surface Science 258 (2012) 9218–9222

Contents lists available at ScienceDirect

Applied Surface Science

journal homepage: www.elsevier.com/locate/apsusc

Antibacterial and surface-enhanced Raman scattering (SERS) activities of AgCl cubes synthesized by pulsed laser ablation in liquid

Chenbo Dong[a,1], Zijie Yan[b,1], Jacklyn Kokx[a], Douglas B. Chrisey[b,*], Cerasela Zoica Dinu[a,**]

[a] Department of Chemical Engineering, West Virginia University, Morgantown, WV 26506, USA
[b] Department of Materials Science and Engineering, Rensselaer Polytechnic Institute, Troy, NY 12180, USA

ARTICLE INFO

Article history:
Available online 9 August 2011

Keywords:
AgCl cubes
E. coli
Antibacterial
Killing capabilities

ABSTRACT

We used pulsed laser ablation in liquid to fabricate silver chloride (AgCl) nanocubes directly from a bulk Ag target in sodium chloride (NaCl) solution. We optimized particle size and investigated the surface properties of the cubes for their Surface Enhanced Raman Scattering (SERS) behavior relative to Rhodamine 6G (R6G). The SERS behavior was related to the surface properties, clearness, and morphology, *i.e.*, varied atomic arrangements and surface energies of different facets of the cubes. In addition, we have demonstrated that our easily synthesized AgCl cubes were antibacterial with a high efficiency to decontaminate *Escherichia coli* upon contact. Our results can be extended to generate particle-based coatings with antibacterial properties.

1. Introduction

Silver-based materials are being used in the development of biological and pharmaceutical processes [1], as coating materials for medical devices [2], for orthopedic or dental graft materials [3], or for water sanitization [4]. Since silver displays multiple modes of inhibitory action to microorganisms [5–7], with the arising and increased resistance of number of microorganism toward multiple antibiotics [8], and continuous emphasis on reducing health cost, research has also focused on developing new types of low cost, effective coatings [9–11]. Recent research has shown that silver chloride (AgCl) exhibits surface enhanced Raman scattering (SERS) capabilities and can be employed for the fabrication of photographic paper and photochromic lenses [12–19]. These capabilities are considered to originate from the controlled shape of Ag clusters formed in the AgCl lattice [13,15,16,18,19], although the surface Ag^+ complexes may also play an important role [12]. The Ag clusters form by a self-sensitization process of AgCl, namely, Ag^+ ions combine with photo-induced electrons to form Ag^0 atoms/clusters upon light irradiation [20]. Despite their large SERS-based applications there had been only few methods available to generate AgCl materials with fine control over their properties for SERS detection. Moreover, to our knowledge, there has been no previous study that combines the inhibitory effects of AgCl with its SERS detection capabilities to generate analytical tools used for detection and decontamination.

AgCl-related materials were synthesized by precipitation reactions between Ag^+ and Cl^- ions via wet chemical methods; the shape of the clusters was controlled when surfactant was used in the preparation [13,16,18,19]. AgCl cubes were fabricated with the use of poly(vinyl pyrrolidone) and further modified into AgCl:Ag by post heat-treatment at elevated temperatures [19]. Recently, AgCl nanocubes fabrication was demonstrated via a simple reaction between silver nitrate ($AgNO_3$) and sodium chloride (NaCl) in ethylene glycol [21]. Our group has shown that excimer laser ablation of Ag target in aqueous solutions of NaCl directly generates AgCl cubes in the absence of surfactant molecules [14]. Pulsed laser ablation in liquid is a technique widely used for nanocrystal fabrication [22,23]. The technique is not only reliable and easily applicable, but also skips additional steps that could lead to surface contaminations thus increasing the potential applications related to surface properties of the synthesized particles. Current research trend in this area is to fabricate functional nanostructures utilizing the merits of this technique [24] with focus on the synthesis of the nanostructure formation and growth. Herein we report for the first time on the antibacterial activity and efficiency of AgCl nanocubes and nanobars prepared by pulsed laser ablation of Ag target in

* Corresponding author at: Department of Materials Science and Engineering, Department of Biomedical Engineering, School of Engineering, Rensselaer Polytechnic Institute, 110 8th Street, Troy, NY, 12180-3590, USA. Tel.: +1 518 276 3303; fax: +1 518 276 8554.
** Corresponding author at: Department of Chemical Engineering, West Virginia University, College of Engineering and Mineral Resources, PO Box 6102, ESB 445, Morgantown, WV, 26506, USA. Tel.: +1 304 293 9338; fax: +1 304 293 4139.
E-mail addresses: chrisd@rpi.edu (D.B. Chrisey), cerasela-zoica.dinu@mail.wvu.edu (C.Z. Dinu).
[1] The authors contributed equally to this work.

0169-4332/$ – see front matter © 2011 Elsevier B.V. All rights reserved.
doi:10.1016/j.apsusc.2011.07.076

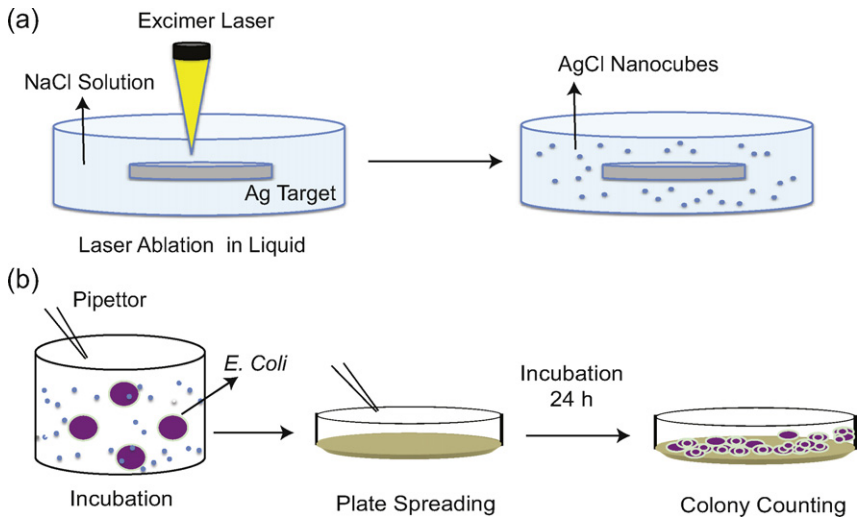

Scheme 1. Concept figure of the AgCl preparation by pulsed laser ablation of Ag target in NaCl solution (a) and their antibacterial testing using standard plating assay and gram negative bacteria (b).

aqueous solutions of NaCl. We also investigate their SERS activities against Rhodamine 6G in order to formulate new analytical tools for detection and decontamination.

2. Materials and methods

2.1. Fabrication and characterization of AgCl cubes

AgCl particles in the form of cubes were fabricated using a laser ablation method previously described [14]. Briefly, a silver target (99.99% pure, Kurt J. Lesker Company, USA) was placed in a rotating glass beaker filled with aqueous solution of 0.005 M NaCl (≥99.0% pure, Mallinckrodt Baker, Inc., USA). A KrF excimer laser with wavelength of 248 nm, pulse width of 30 ns, and repetition frequency of 10 Hz, was focused onto the target surface. Continuous ablation of the target was performed for 20 min at a laser fluence of ~8 J/cm^2. The products were isolated and collected by centrifugation. Purification and re-dispersion steps in Milli-Q water were also employed to remove any residual NaCl. Scanning electron microscopy (SEM) was performed on a JEOL JSM-6330F field emission at 10 kV. X-ray diffraction (XRD) patterns were collected on an X-ray diffractometer (Bruker D8) with Cu Kα radiation.

2.2. Preparation of Escherichia coli (E.coli)

A seed culture of *Escherichia coli* was prepared by inoculating 2×YT media (16 g/L tryptone, 10 g/L yeast extract and 5 g/L NaCl; Fisher Scientific, USA) supplemented with 200 μg/ml ampicillin (Fisher Scientific, USA) and 30 μg/ml chloramphenicol (Fisher Scientific, USA) with a frozen cell stock of *E. coli* BL21 Star (DE3) pLysS cells (Invitrogen, USA). The seed culture was incubated overnight at 37 °C on an orbital shaker and then used to inoculate a main culture of 1 L 2×YT media also supplemented with 200 μg/ml ampicillin and 30 μg/ml chloramphenicol. The main culture was incubated at 37 °C at 250 rpm in a 2 L baffled flask until an optical density at 600 nm (OD600) of 0.6 was reached. Cells were subsequently pelleted by centrifugation at 4500 rpm for 5 min and resuspended in a phosphate buffer solution (PBS, 10 mM, pH 7.5, Dulbecco's Phosphate Buffered Saline, Sigma, USA). This step was repeated at least 3 times to remove all the nutrient media. In order to obtain an approximate measure of cell density in terms of CFU/ml, the adsorption of the bacterial suspension was measured at 600 nm (Absorbance of 1 at 600 nm corresponds to 8×10^8 CFU/ml) [25].

2.3. Antibacterial efficiency of AgCl cubes

To evaluate the antibacterial efficiency of AgCl cubes produced as previously described, a vial containing the cubes (1 mg/ml) was incubated with different concentrations of bactericidal suspensions ($2–5 \times 10^5$ CFU/ml) and placed on a shaker at 300 rpm. For evaluating the kinetics of bactericidal killing, 10 μl solution was withdrawn after 30 min, 1, 3, 6, 12, 18 and 24 h respectively and spread onto a nutrient agar plate. The nutrient agar plates were obtained by poring a sterilized mixture of 1 L Milli-Q water containing nutrient broth (8 g, Difco, USA) and 12 g of Agar (Sigma, USA) in 100 O.D. × 15 mm H Petri dishes (Fisher, USA). The nutrient agar plates were plated with the 10 μl of bacteria or bacteria incubated with AgCl were incubated at 37 °C for 24 h. Bactericidal efficiency was determined by counting colonies grown on the nutrient agar surface and by comparing colony counts obtained after bacteria incubation with AgCl cubes with those obtained from control nutrient agar plates (*i.e.*, where the bacteria was plated without exposure to the AgCl nanocubes). Every experiment was performed in duplicate and five independent sets of experiments were performed per total and for a relevant statistic.

2.4. Bactericidal efficiency of AgCl containing plates

In other experiments, 10 μl of AgCl cubes were incubated in ~20 ml mixture containing nutrient broth and agar (prepared as previously described) at 90 °C. The mixture was pored onto Petri dishes and left to cool down at room temperature. The plates were then incubated with 10 μl *E. coli* solution at 10^5 CFU/ml and the antibacterial efficiency by slow release of the Ag^+ ions was evaluated after incubation of the plates at 37 °C for 24 h. The antibacterial efficiency was reported relative to control experiments (*i.e.*, bacteria grown on nutrient agar plates).

2.5. SERS tests

Several drops of solution containing AgCl cubes were deposited on silicon wafers; the wafer was dried in air and at room temperature. Rhodamine 6G (R6G, 99% pure, Acros Organics, USA) aqueous solutions (concentration of 10^{-11}–10^{-5} M) were then dripped on the AgCl deposits and evaporated. The SERS spectra were recorded with a Renishaw S2000 Raman spectroscope using an argon-ion laser (514.5 nm) and through a 50× microscope objective. The

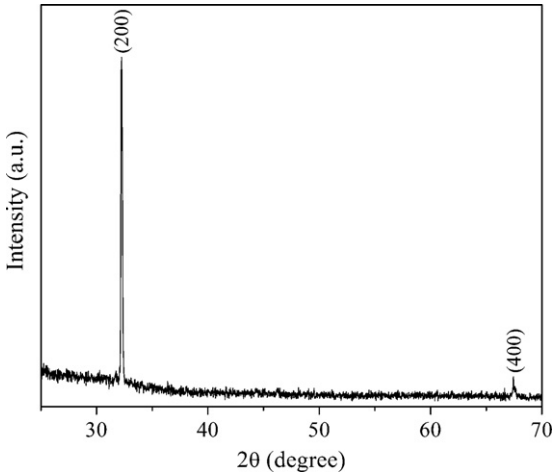

Fig. 1. XRD spectrum of the products fabricated by excimer pulsed laser ablation of Ag target in NaCl solution.

incident laser power was kept at 10% of 50 mW with accumulation time of 10 s.

3. Results and discussions

AgCl particles were prepared using pulsed laser ablation of Ag target in NaCl solution (Scheme 1(a)). To remove any residual NaCl, particles were washed and redispersed by centrifugation and filtration in Milli-Q water. The structure of the laser-produced particles was characterized by XRD. Fig. 1 shows the XRD spectrum; the peaks can be indexed into cubic phase of AgCl (JCPDS card no. 31-1238). The predominance of (2 0 0) and (4 0 0) peaks indicates that the AgCl particles have cubic shapes.

To further confirm the morphology of particles produced by pulsed laser ablation in liquid, we performed SEM analysis (Fig. 2). As shown in Fig. 2(a), the nanoparticles have well-defined cubic morphologies with the edge lengths of the cubes being about 100–200 nm (Fig. 2(b)). The pulsed laser ablated sample also contained nanobars; the arrows in Fig. 2(c) and (d), respectively pointed out five independent nanobars. As shown, the nanobars have different aspect ratios: [1] 1.6, [2] 2.5, [3] 2.6, [4] 3.6, and [5] 6.7, respectively. To our knowledge, no previous demonstration of nanobars was reported. Nanobars could offer unique immobilization nanosupports because of their high volume-surface ratio [26]. Our results also show that smaller nanoparticles seem to have appeared on the surface of the nanobars and nanocubes as revealed by Fig. 2(d). This was previously reported for AgCl under intensive electron beam irradiation, with the irradiation heat partially decomposing the AgCl [14].

As synthesized and purified nanocubes were further tested for their antibacterial properties upon contact with gram negative *E. coli* grown following standards protocols (Scheme 1(b)). Fig. 3(a) shows the atomic force microscopy of the bacterial colonies while the inset shows the 3D image of a single *E. coli* isolated from the culture. The nanocubes were incubated in the bacterial solution; samples were extracted after different incubation periods and plated onto nutrient agar plates. The antibacterial efficiency was reported relative to the control nutrient agar plates, namely plates incubated with non-exposed *E. coli*. Our results showed that there is a considerable decrease in the number of colonies of *E. coli* upon their incubation with the nanocubes (Fig. 3(b)). Visual counting reveals >95% antibacterial efficiency against 10^5 CFU/ml of bacteria in only 3 h incubation, all relative to control samples (Fig. 3(c)).

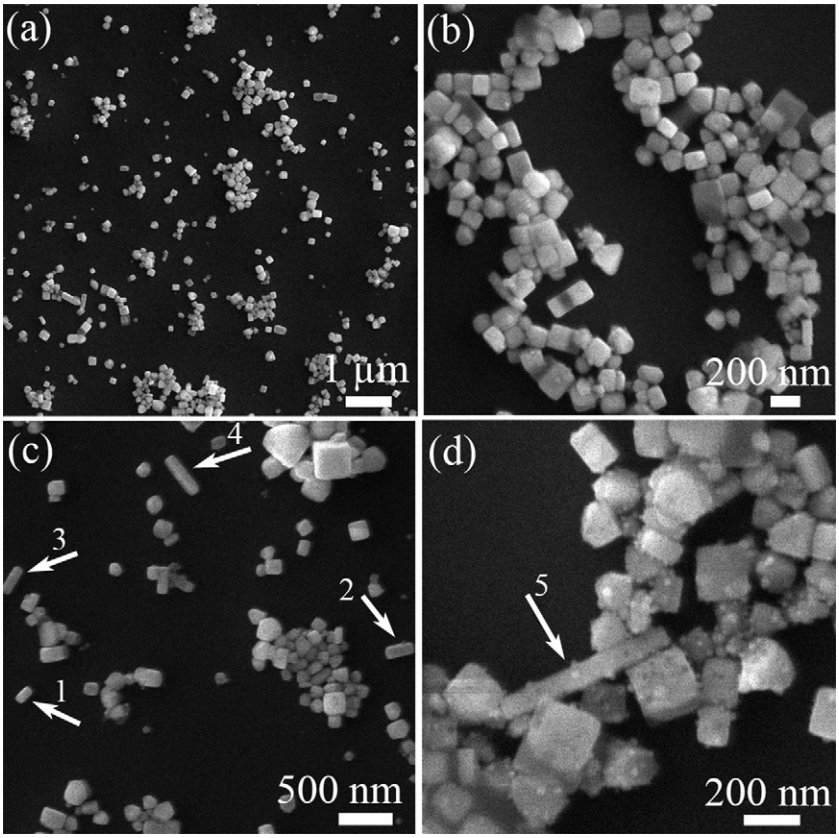

Fig. 2. SEM images of the laser-produced AgCl particles: (a) a general view, (b) magnified image of nanocubes, (c) and (d) nanobars are observed in the products (indicated by the arrows).

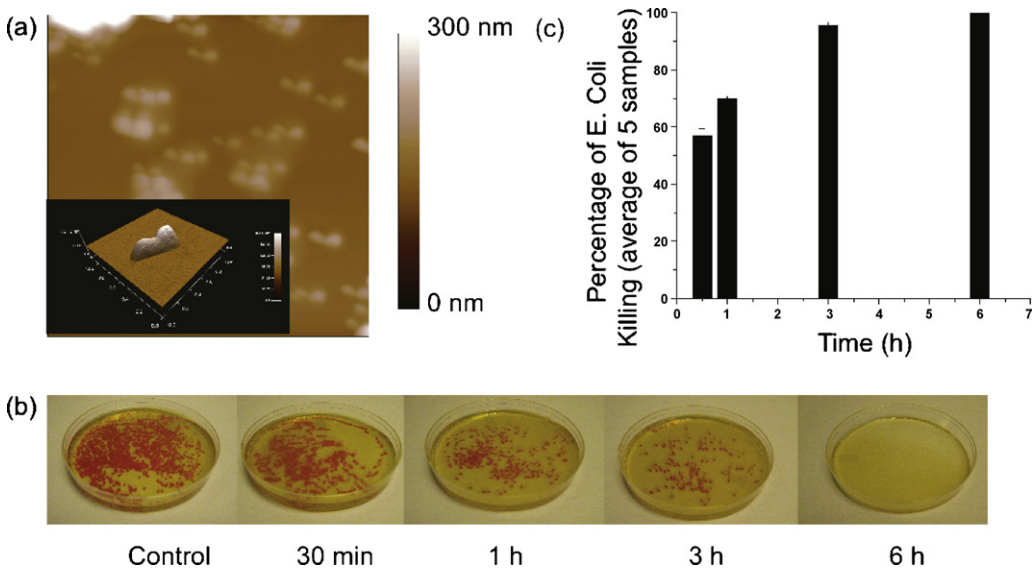

Fig. 3. (a) Atomic force microscopy of the bacterial colonies. Inset: 3D image of a single *E. coli*. (b) Agar plates marked with colonies of bacteria. The number of colonies after different incubation time of bacteria with AgCl is reported relative to control plates. (c) Percentage of *E. coli* killing upon incubation with AgCl for different amount of time.

We correlated the high decontamination capability recorded in our experiments with the shape of the AgCl particles. Specifically, on their {1 0 0} facets these synthesized AgCl nanocubes are either positively or negatively charged and thus active, leading to enhanced bacterial adsorption and thus increased decontamination [27].

The bacterial samples (with or without nanocubes) were also inspected with SEM to further confirm that there were no bacteria left after incubation with AgCl nanocubes. Fig. 4(a) shows bacteria in SEM while Fig. 4(b) identifies nanocubes embedded in cellular debris. To confirm the presence of bacteria or cellular debris and nanocubes, we also used Energy Dispersive X-ray analysis (EDX). The EDX spectra (Fig. 4(a) and (b) inset, respectively) display peaks corresponding to the difference of energy levels for which the most X-rays had been emitted by each individual sample tested; each of these peaks corresponds to a single element in the specimen. As shown, no Ag or Cl peaks were indentified for bacteria (Fig. 4(a) inset), however the spectrum changed to include those elements and others (which were the mark of the cellular debris) upon incubation of bacteria with AgCl.

We suggest that, due to their controlled geometry and capacity for decontamination (as shown by our results), one can use pulsed laser synthesized nanocubes as a contact biocidal compound. We envision incorporating the nanocubes into a polymer or paint matrix that spatially stabilize and physically immobilize them at the surface while the porosity of the matrix will further allow for ion (Ag^+) or small molecule diffusion. Such matrix interactions would further be used for antibacterial decontamination. An interesting capability of such matrix would also permit detection of the decontaminant upon binding.

To test the feasibility of our hypothesis we performed preliminary SERS analysis. The SERS activities of AgCl nanocubes were evaluated by using R6G as probing molecules. Fig. 5 shows the Raman spectra of 10^{-11}–10^{-5} M R6G. On bare Si wafer coated with 10^{-5} M R6G, only a peak at 520 cm^{-1} associating with Si was observed, while on AgCl nanocubes coated with 10^{-5} M R6G, multiple peaks were observed. The observed peaks were identified with the fingerprint features of R6G Raman spectrum [28]. These results indicate that AgCl nanocubes could largely enhance the Raman signal of R6G molecules. We observed that the intensities of the peaks are concentration dependent, with a decrease in the peak intensity being recorded when the R6G concentration decreases. At concentrations of 10^{-7} and 10^{-9} M, only the band peaked at 1598 cm^{-1} dominates, while at 10^{-11} M all the peaks were invisible because much fewer R6G molecules were present on AgCl cubes. This result indicates that the AgCl nanocubes obtained using pulsed laser

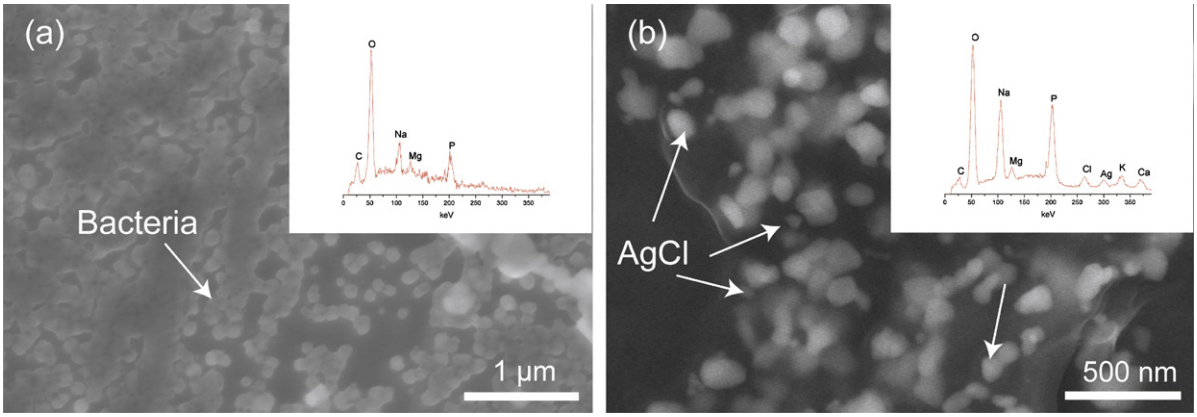

Fig. 4. (a) *E. coli* in SEM (arrows point to selected bacteria). Inset: the EDX spectrum of *E. coli*. (b) AgCl nanocubes embedded into a mass of cellular debris (arrows point to selected nanocubes). Inset: the EDX spectrum of the AgCl embedded in the cellular debris.

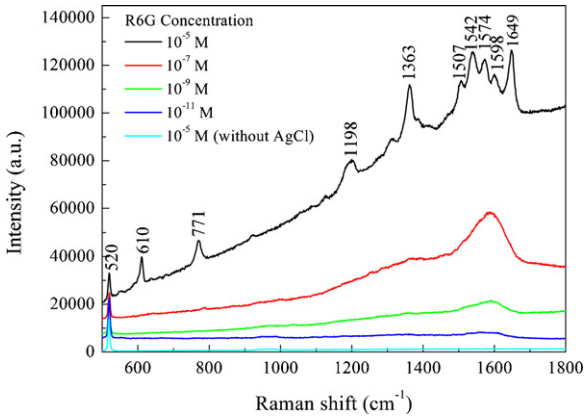

Fig. 5. SERS spectra of R6G on AgCl particles and bare Si wafer (control).

ablation can be used in the analytical environment for routine SERS detection measurements. Further, we also performed preliminary experiments in which we incorporated the nanocubes in nutrient agar plates and tested their decontamination properties by slow release of Ag^+ ions and upon exposure to bacteria. Our results show that for only 5 μg of nanocubes there was 92% killing of *E. coli* by slow release of ions.

Combining AgCl SERS with AgCl antibacterial efficiency and suspending such AgCl nanocubes or nanobars in paint of polymer matrices, would lead to generation of coatings with detection and bactericidal capabilities. Moreover, if deposition by drop-coating or nebulizer spray techniques of AgCl nanocubes onto copper, silicon, and plastic substrates is chosen, one could extend even further the applications of such nanoparticles for detection and decontamination.

4. Conclusions

We have synthesized nanocubes and nanorods of AgCl using a simple and efficient process of pulsed laser ablation in liquid. The synthesized nanocubes possess antibacterial properties with high decontamination capability of gram-negative bacteria, namely *E. coli*. Moreover, as synthesized nanocubes have SERS detection capabilities, that makes them potential candidates for analytical laboratories.

Acknowledgements

The authors thank Adrienne McGraw, WVU/Chemical Engineering for help with SEM and EDX analysis. The work performed in Dr. Dinu lab was supported by the NSF/CBET 1033266, NSF/CMMI 1049150, NSF/EPS-1003907, and WVNano. Work performed in Dr. Chrisey's lab was supported by the NSF/CMMI 1049147.

References

[1] Z. Wang, X. Chen, M. Chen, L. Wu, Facile fabrication method and characterization of hollow Ag/SiO_2 double shelled spheres, Langmuir 7 (2009) 7646–7651.
[2] A. Babapour, B. Yang, S. Bahang, W. Cao, Low-temperature sol-gel-derived nanosilver-embedded silane coating as biofilm inhibitor, Nanotechnology 22 (2011) 155602.
[3] H. Rosengren, A. Dixon, Antibacterial prophylaxis in dermatologic surgery: an evidence-based review, Am. J. Clin. Dermatol. 11 (2010) 35–44.
[4] B. De Gusseme, T. Hennebel, E. Christiaens, H. Saveyn, K. Verbeken, J.P. Fitts, N. Boon, W. Verstraete, Virus disinfection in water by biogenic silver immobilized in polyvinylidene fluoride membranes, Water Res. 45 (2011) 1856–1864.
[5] R.T. Carbon, S. Lugauer, U. Geitner, A. Regenfus, M. Boswald, J. Greil, T. Bechert, S.I. Simon, H.P. Hummer, J.P. Guggenbichler, Reducing catheter-associated infections with silver-impregnated catheters in long-term therapy of children, Infection 27 (Suppl. 1) (1999) S69–S73.
[6] J.P. Guggenbichler, M. Boswald, S. Lugauer, T. Krall, A new technology of microdispersed silver in polyurethane induces antimicrobial activity in central venous catheters, Infection 27 (Suppl. 1) (1999) S16–S23.
[7] P.L. Tran, A.A. Hammond, T. Mosley, J. Cortez, T. Gray, J.A. Colmer-Hamood, M. Shashtri, J.E. Spallholz, A.N. Hamood, T.W. Reid, Organoselenium coating on cellulose inhibits the formation of biofilms by *Pseudomonas aeruginosa* and *Staphylococcus aureus*, Appl. Environ. Microbiol. 75 (2009) 3586–3592.
[8] C.P. Andam, G.P. Fournier, J.P. Gogarten, Multi-level populations and the evolution of antibiotic resistance through horizontal gene transfer, FEMS Microbiol. Rev. (2011).
[9] R. Dastjerdi, M. Montazer, S. Shahsavan, A novel technique for producing durable multifunctional textiles using nanocomposite coating, Colloids Surf. B: Biointerfaces 81 (2010) 32–41.
[10] R. Dastjerdi, M. Montazer, A review on the application of inorganic nanostructured materials in the modification of textiles: focus on anti-microbial properties, Colloids Surf. B: Biointerfaces 79 (2010) 5–18.
[11] S.D. Gittard, R.J. Narayan, C. Jin, A. Ovsianikov, B.N. Chichkov, N.A. Monteiro-Riviere, S. Stafslien, B. Chisholm, Pulsed laser deposition of antimicrobial silver coating on Ormocer microneedles, Biofabrication 1 (2009) 041001.
[12] L. Dawei, W. Jian, X. Houwen, S. Xu, L. Fan-chen, Enhancement origin of SERS from pyridine adsorbed on AgCl colloids, Spectrochim. Acta, Part A 43 (1987) 379–382.
[13] M. Volkan, D.L. Stokes, T. Vo-Dinh, A sol-gel derived AgCl photochromic coating on glass for SERS chemical sensor application, Sens. Actuators, B 106 (2005) 660–667.
[14] Z. Yan, G. Compagnini, D.B. Chrisey, Generation of AgCl Cubes by excimer laser ablation of bulk Ag in aqueous NaCl solutions, J. Phys. Chem. C 115 (2010) 5058–5062.
[15] Y.Y. Li, Y. Ding, Porous AgCl/Ag nanocomposites with enhanced visible light photocatalytic properties, J. Phys. Chem. C 114 (2010) 3175–3179.
[16] P. Wang, B.B. Huang, Z.Z. Lou, X.Y. Zhang, X.Y. Qin, Y. Dai, Z.K. Zheng, X.N. Wang, Synthesis of highly efficient Ag@AgCl plasmonic photocatalysts with various structures, Chem. Eur. J. 16 (2010) 538–544.
[17] B. Tomsic, B. Simoncic, B. Orel, M. Zerjav, H. Schroers, A. Simoncic, Z. Samardzija, Antimicrobial activity of AgCl embedded in a silica matrix on cotton fabric, Carbohydr. Polym. 75 (2009) 618–626.
[18] P. Wang, B. Huang, X. Qin, X. Zhang, Y. Dai, J. Wei, M.-H. Whangbo, Ag@AgCl: a highly efficient and stable photocatalyst active under visible light, Angew. Chem. Int. Ed. 47 (2008) 7931–7933.
[19] C.H. An, S.N. Peng, Y.G. Sun, Facile synthesis of sunlight-driven AgCl:Ag plasmonic nanophotocatalyst, Adv. Mater. 22 (2010) 2570–2574.
[20] K. Pfanner, N. Gfeller, G. Calzaferri, Photochemical oxidation of water with thin AgCl layers, J. Photochem. Photobiol., A 95 (1996) 175–180.
[21] C. An, S. Peng, Y. Sun, Facile synthesis of sunlight-driven AgCl:Ag plasmonic nanophotocatalyst, Adv. Mater. 22 (2010) 2570–2574.
[22] G.W. Yang, Laser ablation in liquids: applications in the synthesis of nanocrystals, Prog. Mater. Sci. 52 (2007) 648–698.
[23] X.Z. Lin, P. Liu, J.M. Yu, G.W. Wang, Synthesis of CuO nanocrystals and sequential assembly of nanostructures with shape-dependent optical absorption upon laser ablation in Liquid, J. Phys. Chem. C 113 (2009), 17543-17547.
[24] P. Liu, H. Cui, C.X. Wang, G.W. Yang, From nanocrystal synthesis to functional nanostructure fabrication: laser ablation in liquid, Phys. Chem. Chem. Phys. 12 (2010) 3942–3952.
[25] T. Christensen, K. Trabbic-Carlson, W. Liu, A. Chilkoti, Purification of recombinant proteins from *Escherichia coli* at low expression levels by inverse transition cycling, Anal. Biochem. 360 (2007) 166–168.
[26] C.Z. Dinu, S.S. Bale, G. Zhu, J.S. Dordick, Tubulin encapsulation of carbon nanotubes into functional hybrid assemblies, Small 5 (2009) 310–315.
[27] X. Wang, H. Wu, Q. Kuang, R. Huang, Z. Xie, L. Zheng, Shape-dependent antibacterial activities of Ag_2O polyhedral particles, Langmuir 26 (2009) 2774–2778.
[28] L. Lu, A. Kobayashi, K. Tawa, Y. Ozaki, Silver nanoplates with special shapes: controlled synthesis and their surface plasmon resonance and surface-enhanced raman scattering properties, Chem. Mater. 18 (2006) 4894–4901.